Volume 6, Number 1, January 2012 ISSN 1881-803X

ICIC Express Letters

An International Journal of Research and Surveys

Editors-in-Chief
Yan Shi, Tokai University, Japan
Junzo Watada, Waseda University, Japan

Indexed by *Ei Compendex (Elsevier)*
Scopus (Elsevier)
INSPEC (IET)

Published by ICIC International
http://www.ijicic.org/icicel.htm

ICIC EXPRESS LETTERS

Volume 6, Number 1, January 2012

CONTENTS (*Continued*)

 ISSN 1881-803X Printed in Japan

ICIC Express Letters
Volume **6**, Number **1**, January **2012**

ICIC International ©2012 ISSN 1881-803X
pp. 281–287

OPTIMAL PATH PLANNING FOR MOBILE ROBOT IN CONSIDERATION OF ROAD ATTRIBUTES

Fei Liu, Shan Liang*, Xiaodong Xian and Huibo Bi

College of Automation
Chongqing University
No. 174, Shazhengjie, Shapingba District, Chongqing 400044, P. R. China
*Corresponding author: lightsun@cqu.edu.cn

Received April 2011; accepted July 2011

Abstract. *This paper proposes a strategy of optimal path planning for mobile robot in outdoor environment in consideration of road attributes, which comprise path length, surface roughness and road grade. The road in the environment is partitioned into multiple segments, and for each one the mode of the cost (energy consumption) that the robot will pay for is established under the constraints of the attributes. The path accessible to the goal is constituted by a part of segments and its cost is defined to be the sum of the cost of each segment. By comparing the total cost of each path, the optimal one with minimum cost is determined. After measuring the parameter values in the model experimentally, we carry out the simulation, where the superiority and important practical significance are shown by the comparison with traditional methods.*
Keywords: Mobile robot, Path planning, Road attributes, Surface roughness, Road grade

1. **Introduction.** Autonomous mobile robots have vast applications in reality, such as automatic welding in a production line [1], transporting in a warehouse [2], guiding working in a museum [3] and automatic patrolling in a transformer substation [4]. For each application, energy is the potential to perform work, without which the robot will become immobilized and useless [5, 6]. Typically, rechargeable batteries can only provide few hours of peak usage, e.g., with a battery pack, a Honda humanoid robot can run for only 30 mins [7]. Therefore, to minimize energy consumption, the optimal path planning for going to a goal from a start point becomes important for mobile robot in outdoor environment, and this issue attracts much concerns.

The majorities of path planning algorithms seek to find a path with shortest Euclidean length based on pre-scanned map [8, 9, 10, 11], where the path length is regarded as the criterion for evaluating a path. While the complex features of outdoor environment are considered, the criterion of path length is no longer suitable for determining an optimal path [12]. When terrain characteristics such as inclination or surface roughness are taken into account, some researches investigate the minimum weighted paths planning based on weighted polygonal subdivisions [13], on weighted polyhedral surfaces [14], or weighted regions [15], etc. However, the weight is just used as a parameter for theoretical analysis, and no concrete analysis is involved. In addition, by defining the cost of a path to be the energy consumed due to both friction and gravity, Sun et al. focused on planning energy-minimizing path using terrain map [16]. However, the environment aimed is the huge wild area (e.g., a river basin referred in the article), so a number of constraints are employed, and this increases the complexity of computing inevitably. In addition, Mei et al. discussed the most energy-efficient path planning [17]. However, it focuses on the discussion about the energy spent on robot's turning and rotating, while the terrain characteristics are not considered. Furthermore, Guo et al. adopted the terrain roughness

and terrain slope to define the power consumption, but it limits to qualitative analysis, no experiment is executed for quantitative analysis [18].

In Figure 1, we show three typical situations in outdoor environment compared with indoor environment. Based on these situations, in this study, the road attributes including length, road surface roughness and road grade are taken into account to plan the optimal path. First, we model the working environment and describe the path in detail. Then the energy consumption model is built on basis of force analysis of a robot moving on road. Finally, simulation is given to prove the effectiveness and advantage of our approach by comparison with traditional methods.

(a) Walking on a flat road (b) Walking on a rough road (c) Walking on a slope

FIGURE 1. Three typical situations in outdoor environment

2. **Model of Working Environment and Forces Analysis of Mobile Robot.** Here, a metric-topological map is used to describe the working environment, as shown in Figure 2. There are some assumptions: The road is partitioned into M segments. Each segment P_m $(m = 0, 1, \ldots, M-1)$ has three attributes: p_{ml}, p_{mr} and p_{mg}, where p_{ml} (unit: m) represents the length of P_m, p_{mr} (unit: m/km) is the surface roughness, and p_{mg} (unit: rad) is the actual road grade of P_m, and $-\pi/2 < p_{mg} < \pi$. Specially, the sign of p_{mg} is determined by the coordinates of the two endpoints. In the coordinate system shown in Figure 2, for P_m, $A(x, y)$ represents one endpoint with smaller abscissa value or smaller ordinate value and the same abscissa value with the other one. The other endpoint is named as $B(x, y)$. According to the longitudinal robot model shown in Figure 3, the sign of p_{mg} is decided by

$$\begin{cases} p_{mg} \geq 0, & A(x,y) \text{ corresponds to } A' \text{ actually} \\ p_{mg} < 0, & B(x,y) \text{ corresponds to } B' \text{ actually} \end{cases}. \tag{1}$$

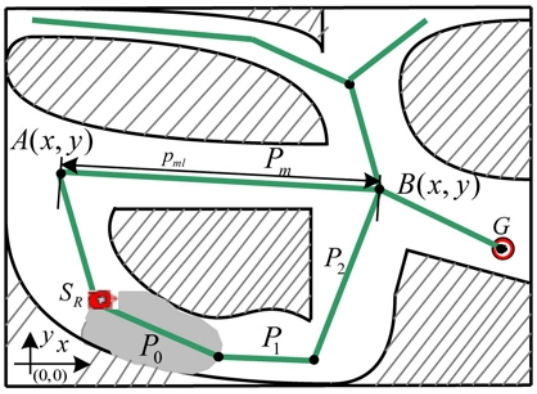

FIGURE 2. Model of the working environment

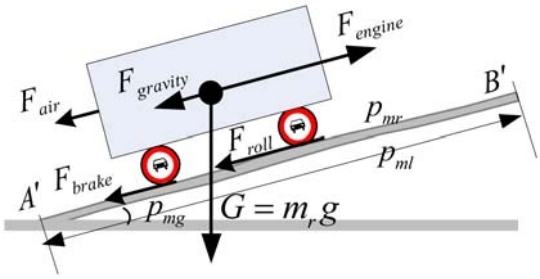

FIGURE 3. The force analysis of a mobile robot walking on road

According to Figure 3, the robot is constrained by five forces, which are the engine force F_{engine}, the rolling resistance F_{roll}, the brake force F_{brake}, the air drag F_{air} and the gravity induced force $F_{gravity}$ respectively [19]. Given a robot walking at low speed and without braking, we assume that

$$\begin{cases} F_{air} = 0 \\ F_{brake} = 0 \end{cases}, \tag{2}$$

thus, F_{roll} can be expressed as

$$F_{roll} = \gamma_r m_r g \cos(p_{mg}), \tag{3}$$

where γ_r is the coefficient of rolling resistance that is proportional to p_{mr}. Let ρ ($\rho > 0$) be the proportion, namely, $\gamma_r = \rho p_{mr}$, then

$$F_{roll} = \rho p_{mr} m_r g \cos(p_{mg}). \tag{4}$$

In addition, $F_{gravity}$ is induced by gravity G, and the relation between $F_{gravity}$ and p_{mg} is

$$F_{gravity} = m_r g \sin(p_{mg}), \tag{5}$$

where m_r is the weight of the robot and g is the gravitational constant.

Assume that the robot walks at a constant velocity, that is to say, the acceleration is zero, and then we obtain

$$F_{engine} = F_{roll} + F_{gravity}. \tag{6}$$

3. Implementation of Optimal Path Planning.

This section will build the model of energy consumption first, and then describe the implementation of our strategy of optimal path planning.

3.1. Model of energy consumption.

Define $W_{p_{ml}}$ as the total work the robot does when moving for distance p_{ml} dragged by F_{engine}, then we have

$$W_{p_{ml}} = F_{engine} p_{ml} = (F_{roll} + F_{gravity}) p_{ml}. \tag{7}$$

According to (4) and (5) additionally, we obtain

$$W_{p_{ml}} = \rho p_{mr} m_r g \cos(p_{mg}) p_{ml} + m_r g \sin(p_{mg}) p_{ml}. \tag{8}$$

The energy the robot needs to drive motors is provided by batteries. Define C as the energy consumption for passing segment P_m, and we call it the cost the robot will pay for. Approximately, C is proportional to $W_{p_{ml}}$, namely, $C \propto W_{p_{ml}}$, then we can describe C using $W_{p_{ml}}$ and a positive coefficient λ as $C = \lambda W_{p_{ml}}$. In addition, we define r_C (unit: V/m) as the energy consumption rate, which means the average voltage decrease (unit: V) of passing per meter long road. Hence, for passing a segment P_m of attribute p_{ml}, C is calculated to be

$$C = r_C p_{ml}. \tag{9}$$

With (8), we obtain

$$r_C = \rho p_{mr} \lambda m_r g \cos(p_{mg}) + \lambda m_r g \sin(p_{mg}). \tag{10}$$

Let $\kappa = \lambda m_r g$, then (10) becomes

$$r_C = \kappa \rho p_{mr} \cos(p_{mg}) + \kappa \sin(p_{mg}). \tag{11}$$

In the following, two situations are analyzed in terms of p_{mg} and p_{mr}:
(a). $p_{mg} = 0$ and $p_{mr} = \mu_f$. First, with given values $p_{mg} = 0$ and $p_{mr} = \mu_f$ that is constant, and according to (11) we obtain the energy consumption rate $r_{C\_\mu_f}$ of this situation:

$$r_{C\_\mu_f} = \kappa \rho \mu_f. \tag{12}$$

Define $r_{C\_p_{mr}}$ as the energy consumption rate for passing any segment P_m of $p_{mg} = 0$ and p_{mr}, then with (12) we have

$$r_{C\_p_{mr}} = \kappa \rho p_{mr} = \frac{p_{mr}}{\mu_f} r_{C\_\mu_f}. \tag{13}$$

(b). $p_{mg} = \varphi_g$ ($\varphi_g \neq 0$) and $p_{mr} = \mu_f$. Define $r_{C\_\mu_f \varphi_g}$ as the energy consumption rate for a segment of $p_{mg} = \varphi_g$ and $p_{mr} = \mu_f$, with (11) we have

$$r_{C\_\mu_f \varphi_g} = \kappa \rho \mu_f \cos \varphi_g + \kappa \sin \varphi_g. \tag{14}$$

With (12) and (13), we have

$$\kappa \sin \varphi_g = r_{C\_\mu_f \varphi_g} - r_{C\_\mu_f} \cos \varphi_g, \tag{15}$$

thus, for any segment having attributes p_{mg} and p_{mr}, according to (11)-(15), we obtain

$$r_C = \frac{r_{C\_\mu_f}}{\mu_f} p_{mr} \cos(p_{mg}) + \frac{r_{C\_\mu_f \varphi_g} - r_{C\_\mu_f} \cos \varphi_g}{\sin(\varphi_g)} \sin(p_{mg}), \tag{16}$$

then, the energy consumption C for passing segment P_m is

$$C = \frac{r_{C\_\mu_f}}{\mu_f} p_{mr} \cos(p_{mg}) p_{ml} + \frac{r_{C\_\mu_f \varphi_g} - r_{C\_\mu_f} \cos \varphi_g}{\sin(\varphi_g)} \sin(p_{mg}) p_{ml}. \tag{17}$$

If $r_{C\_\mu_f}$ and $r_{C\_\mu_f \varphi_g}$ are measured experimentally with given values μ_f and φ_g, then C can be obtained for passing any segment of attributes p_{ml}, p_{mg} and p_{mr}.

3.2. **Determining the optimal path.** Assume that there are H different paths from start point to goal, for each path, we note it as R_h ($h = 0, 1, \ldots, H-1$). If R_h is constituted by G ($0 < G \leq M$) segments, and assume that the order is $P_0, P_1, \ldots, P_g, \ldots, P_{G-1}$, then we express R_h as

$$R_h = \{P_0, P_1, \ldots, P_g, \ldots, P_{G-1}\}. \tag{18}$$

For each segment P_g ($g = 0, 1, \ldots, G-1$), we note its cost as C_{P_g}; therefore, the total cost C_{R_h} of R_h is the sum of C_{R_g} ($g = 0, 1, \ldots, G-1$):

$$C_{R_h} = \sum_{g=0}^{G-1} C_{p_g}. \tag{19}$$

Thus, we can select out the optimal path R_{OP} ($OP \in (0, 1, \ldots, H-1)$) by

$$C_{R_{OP}} = \min\{C_{R_h} | h = 0, 1, \ldots, H-1\}, \tag{20}$$

where $C_{R_{OP}}$ is the cost of R_{OP}.

4. **Determination of the Values of $r_{C\_\mu_f}$ and $r_{C\_\mu_f\varphi_g}$.** This section will measure the values of parameters $r_{C\_\mu_f}$ and $r_{C\_\mu_f\varphi_g}$ by experiments.

Assume that V_{start} is the voltage value when the robot begins to work, and V_{end} the value after walking at the average speed $\overline{v}$ for a period of time $\overline{t}$, then

$$r_C = \frac{V_{start} - V_{end}}{\overline{v}\overline{t}}. \tag{21}$$

In this paper, the road surfaces are divided into only two kinds, i.e., the flat surface and the rough surface, which are shown in Figure 1(a) and Figure 1(b) respectively. We use μ_f and μ_r to describe the surface roughness of these two surfaces respectively.

A Pioneer 3-AT robot produced by MobileRobots Inc. is utilized in the experiments. Three lead acid cells are employed to provide energy in this robot [20], and the full voltage V_{full} is measured to be $12.7V$ approximately. According to the practical situation, the threshold voltage V_{low} warning the robot to return for recharging is set to be $11.3V$. In the experiments, the robot starts to run at full voltage and keeps running at the average speed of $\overline{v} = 0.75m/s$ till the voltage value decreases to $11.3V$. After testing many times on a flat road of $p_{mg} = 0$ and $p_{mr} = \mu_f$, the average continuous running time $\overline{t_f}$ is measured to be about 2.67 hours, hence,

$$r_{C\_\mu_f} = \frac{12.7V - 11.3V}{0.75m/s \times 2.67h \times 3600s/h} \approx 0.1942 \times 10^{-3}V/m. \tag{22}$$

The same test procedures are repeated on the rough road of $p_{mr} = \mu_r$, and we get $\overline{t_r} \approx 2.07h$, therefore,

$$r_{C\_\mu_r} = \frac{12.7V - 11.3V}{0.75m/s \times 2.07h \times 3600s/h} \approx 0.2505 \times 10^{-3}V/m. \tag{23}$$

Thus, according to (13), the relation between μ_f and μ_r is

$$\mu_r = \frac{r_{C\_\mu_r}}{r_{C\_\mu_f}}\mu_f = \frac{0.2505 \times 10^{-3}}{0.1942 \times 10^{-3}}\mu_f \approx 1.2899\mu_f. \tag{24}$$

In addition, we do the similar experiments on a slope of $p_{mr} = \mu_f$, road grade $\varphi_g \approx 0.087rad$ and length $L = 100m$. The robot is running uphill with the average speed of $\overline{v} = 0.75m/s$. After testing several times, we get the mean value of $r_{C\_\mu_f\varphi_g}$:

$$r_{C\_\mu_f\varphi_g} \approx 0.2034 \times 10^{-3}V/m. \tag{25}$$

5. **Simulation, Results and Discussion.** According to the real environment, we build a topological map $\mathcal{G}$ shown in Figure 4. In addition, the attributes of all the 24 segments are collected in Table 1.

TABLE 1. The attributes of each segment P_m $(m = 0, 1, \ldots, 23)$ in the working environment

P_m	(p_{ml}, p_{mr}, p_{mg})	P_m	(p_{ml}, p_{mr}, p_{mg})	P_m	(p_{ml}, p_{mr}, p_{mg})
P_0	$(119.6, \mu_f, 0)$	P_8	$(83.0, \mu_f, 0)$	P_{16}	$(100.2, \mu_r, 0)$
P_1	$(155.0, \mu_f, 0.05)$	P_9	$(96.9, \mu_f, -0.06)$	P_{17}	$(84.2, \mu_f, 0)$
P_2	$(119.0, \mu_r, 0)$	P_{10}	$(150.7, \mu_r, -0.09)$	P_{18}	$(124.1, \mu_f, 0)$
P_3	$(97.5, \mu_f, 0)$	P_{11}	$(48.8, \mu_r, 0.52)$	P_{19}	$(124.0, \mu_f, 0)$
P_4	$(71.0, \mu_f, 0.18)$	P_{12}	$(117.4, \mu_f, 0.21)$	P_{20}	$(115.2, \mu_f, 0)$
P_5	$(75.3, \mu_f, 0)$	P_{13}	$(102.0, \mu_f, 0.08)$	P_{21}	$(84.6, \mu_f, -0.09)$
P_6	$(75.3, \mu_f, 0)$	P_{14}	$(53.2, \mu_r, 0.21)$	P_{22}	$(116.0, \mu_f, -0.07)$
P_7	$(84.2, \mu_f, 0.12)$	P_{15}	$(101.9, \mu_f, 0.16)$	P_{23}	$(119.0, \mu_f, -0.08)$

In the simulation, the robot will go to G_R (point I in $\mathcal{G}$) from the start point S_R (point B in $\mathcal{G}$). According to $\mathcal{G}$, 102 different accessible paths from S_R to G_R can be figured

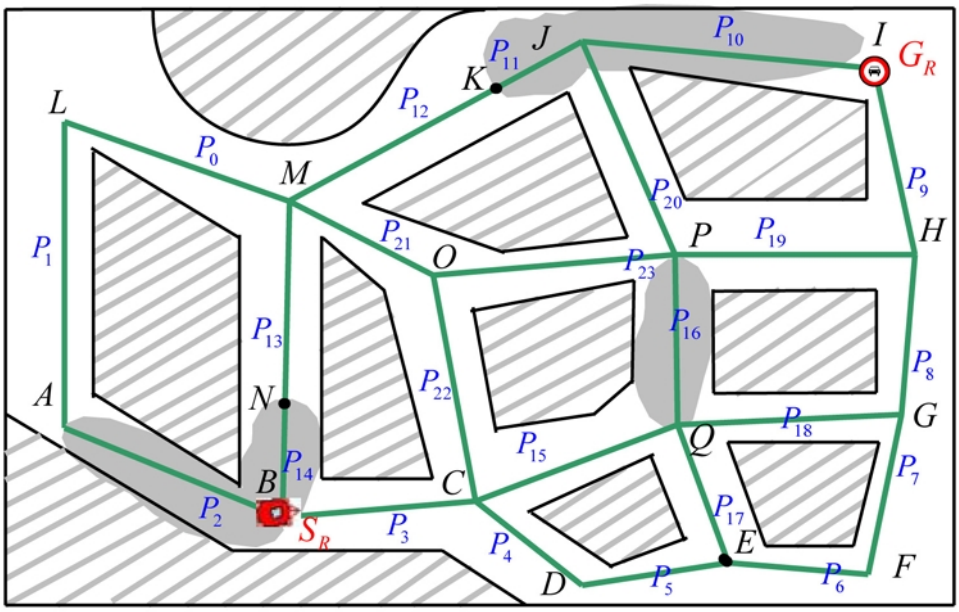

FIGURE 4. The topological map of the working environment

out. After comparing the total cost of each path, we select out the former six paths with minor cost, and list them in Table 2. At the same time, the sequence of the segments which constitute each path is listed, as well as the respective total length (noted as L_T).

TABLE 2. The comparison of six paths

R_h	Sequence of R_h	C/V	L_T/m
R_0	$\{P_3, P_{15}, P_{18}, P_8, P_9\}$	0.0967	503.4
R_1	$\{P_2, P_{22}, P_{23}, P_{19}, P_9\}$	0.1079	553.4
R_2	$\{P_3, P_{15}, P_{16}, P_{19}, P_9\}$	0.1089	520.5
R_3	$\{P_{14}, P_{13}, P_{12}, P_{11}, P_{10}\}$	0.1095	472.1
R_4	$\{P_{14}, P_{13}, P_{21}, P_{23}, P_{19}, P_9\}$	0.1177	579.7
R_5	$\{P_3, P_{22}, P_{23}, P_{20}, P_{10}\}$	0.1228	598.4

According to Table 2, the optimal path is obviously R_0 because it has the minimum cost $0.0967V$; however, this path is not the shortest one. In reality, R_3 has the minimum length $472.1m$, but its cost is even bigger than the cost of R_0, R_1 and R_2, whose length are all longer. Taking R_0 and R_3 as examples, if R_3 is chosen as the optimal path, it actually will cost more energy, and the extra cost is $\Delta C = 0.1095V - 0.0967V = 0.0128V$. As a result, if a week, a month, a year or a longer period of time is considered, the amount of saved energy will be more considerable. This shows the important practical significance of this strategy.

6. **Conclusions.** This paper has proposed a strategy of optimal path-planning for mobile robot in outdoor environment in consideration of multi-attributes of path. We give the simulation and analyze the results by comparing with the traditional method. The results show the superiority and the important practical significance of our strategy. In further research, we will put more emphasis on modifying the values of parameters experimentally to perfect the mathematical models. In addition, we will consider another important issue that the influence of vibration on robot induced by motion. We realize that the continuous vibration may cause the robot to be repaired, which is not what we expected. Further, we will apply this strategy to our patrol robot that works in a transformer substation.

Acknowledgment. This research was sponsored by Project No. CDJXS11171158 Supported by the Fundamental Research Funds for the Central Universities and the Key Project of Science and Technology Committee of Chongqing (CSTC, 2009AB2139).

REFERENCES

[1] O. Madsen, C. B. Sørensen, R. Larsen, L. Overgaard and N. J. Jacobsen, A system for complex robotic welding, *Industrial Robot: An International Journal*, vol.29, no.2, pp.1127-131, 2002.

[2] T. Kesavadas, *Automated Guided Vehicles/Self Guided Vehicles*, http://wings.buffalo.edu/eng/mae/courses/460-564/AGV.pdf, 2007.

[3] A. Chella and I. Macaluso, The perception loop in CiceRobot, a museum guide robot, *Neurocomputing*, vol.72, no.4-6, pp.760-766, 2009.

[4] K. Wang, S. Liang, H. Bi and X. Xian, Implementation of a robot inspection system for substation equipment based on pioneer 3-at, *ICIC Express Letters, Part B: Applications*, vol.2, no.1, pp.221-226, 2011.

[5] Y. G. Mei, Y. H. Lu, Y. C. Hu and C. S. G. Lee, Deployment of mobile robots with energy and timing constraints, *IEEE Transactions on Robotics*, vol.22, no.3, pp.507-522, 2006.

[6] M. C. Silverman, D. Nies, B. Jung and G. S. Sukhatme, Staying alive: A docking station for autonomous robot recharging, *IEEE International Conference on Robotics and Automation*, Washington, D.C., USA, pp.1050-1055, 2002.

[7] R. Aylett, *Robots: Bringing Intelligent Machines to Life*, 1st Edition, Barron's Educational Series, 2002.

[8] T. Hellstrom and O. Ringdahl, Real-time path planning using a simulator-in-the-loop, *International Journal of Vehicle Autonomous Systems*, vol.7, pp.56-72, 2009.

[9] R. Iraji, Robot path planning using wavefront approach with wall-following, *The 2nd IEEE International Conference on Computer Science and Information Technology*, Beijing, China, pp.417-420, 2009.

[10] L. Tian and C. Collins, An effective robot trajectory planning method using a genetic algorithm, *Mechatronics*, vol.14, pp.455-470, 2004.

[11] K.-L. Su, C.-Y. Chung, Y.-L. Liao and J.-H. Guo, Searching algorithm based path planning of mobile robots, *ICIC Express Letters, Part B: Applications*, vol.2, no.1, pp.273-278, 2011.

[12] Z. Sun and J. H. Reif, On finding energy-minimizing paths on terrains, *IEEE Trans. on Robotics*, vol.21, no.1, pp.102-114, 2005.

[13] O. Daescu, J. S. B. Mitchell, S. Ntafos, J. D. Palmer and C. K. Yap, An experimental study of weighted k-link shortest path algorithms, *Proc. of WAFR'2006*, New York, USA, pp.187-202, 2006.

[14] L. Aleksandrov, A. Maheshwari and J. R. Sack, Determining approximate shortest paths on weighted polyhedral surfaces, *Journal of the ACM*, vol.51, no.1, pp.25-53, 2005.

[15] Z. Sun and J. Reif, Adaptive and compact discretization for weighted region optimal path finding, *Fundamentals of Computation Theory*, Durham, vol.2751, pp.13-55, 2003.

[16] Z. Sun and J. H. Reif, On energy-minimizing paths on terrains for a mobile robot, *IEEE International Conference on Robotics and Automation*, Taipei, pp.3782-3788, 2003.

[17] Y. G. Mei, Y. H. Lu, C. S. G. Lee and Y. C. Hu, Energy-efficient mobile robot explo-ration, *Proc. of the 2006 IEEE International Conference on Robotics and Automation*, Orlando, FL, USA, pp.505-511, 2006.

[18] Y. Guo, L. E. Parker, J. David and Z. Y. Dong, Performance-based rough terrain navigation for nonholonomic mobile robots, *The 29th Annual Conference of the IEEE Industrial Electronics Society*, VA, USA, pp.2881-2886, 2003.

[19] P. Sahlholma and K. H. Johansson, Road grade estimation for look-ahead vehicle control using multiple measurement runs, *Control Engineering Practice*, no.18, pp.1328-1341, 2010.

[20] MobileRobots Inc., *Pioneer3 Operations Manual*, http://www.ist.tugraz.at/_attach/Publish/Kmr06/pioneer-robot.pdf, 2006.